Ion energy distribution functions in a supersonic plasma jet

2014 J. Phys.: Conf. Ser. 550 012043

(http://iopscience.iop.org/1742-6596/550/1/012043)

Ion energy distribution functions in a supersonic plasma jet

S Caldirola[1], H E Roman[1] and C Riccardi[1]

[1] Dipartimento di Fisica G. Occhialini, Università degli Studi di Milano-Bicocca, piazza della Scienza 3, I-20126 Milano, Italy

E-mail: claudia.riccardi@mib.infn.it

Abstract. Starting from experimental measurements of ion energy distribution functions (IEDFs) in a low pressure supersonic plasma jet, we propose a model to simulate them numerically from first principles calculations. Experimentally we acquired IEDFs with a quadrupole mass spectrometer (QMS) collecting the argon ions produced from a inductively coupled plasma (ICP) and driven into a supersonic free gas expansion. From the discussion of these results and the physics of our system we developed a simulation code. Integrating the equations of motion the code evolves the trajectory of a single ion across the jet. Ar^+-Ar collisions are modelled with a 12-4 Lennard-Jones potential which considers induced dipole interactions. IEDFs were simulated at different positions along the jet and compared with the experimental data showing good agreement. We have also implemented a charge transfer mechanism in which the ion releases its charge to a neutral atom which can take place at sufficiently close distances and is a function of the impact energy.

1. Introduction

Ion bombardment is a phenomenon inherent in many different thin film deposition processes involving plasma sources. Charged particles can be accelerated onto the substrate surface influencing the formation and growth of thin films. Their energy may modify the substrate surface and temperature enhancing chemical reactions on the surface, growth and nucleation [1-4]. Usually high energetic particles are ions formed in a plasma: argon is the most common gas used for plasma formation and processing since it is the least expensive inert gas. To understand and characterize the effects of these energetic particles it is of fundamental interest the study of their energies. The energy of ions arriving at the substrate is usually much higher than the thermal energy, since it depends on the voltage across the plasma sheath and whether the ions undergo collisions crossing this sheath. The study of ion energy distribution functions (IEDF) is relevant for every plasma processing applications [5-9].

Combining a reactive inductively coupled plasma (ICP) with a supersonic jet, we developed a new approach for thin films deposition: plasma assisted supersonic jet deposition (PA-SJD), which was employed for Titanium dioxide thin film fabrication having a desired morphology [10]. However, the role of ions in PA-SJD is not completely understood yet. Our experimental set-up is made of two different vacuum chambers, in the first a high density Ar-O_2 cold plasma is created. This vacuum chamber is connected through a nozzle to the deposition chamber, the latter kept at a lower pressure. The pressure ratio between the two chambers is set sufficiently

large to generate a supersonic under-expanded jet which drives neutral particles onto a substrate placed along the jet [11].

In this work we study a simple argon plasma. Argon ions are generated inside the first chamber and are then driven inside the deposition chamber by the neutral argon gas flow and accelerated by the potential difference. Our goal is to understand the collisional processes which take place along the supersonic jet and to characterize the IEDFs which influence our depositions. Experimentally we acquired IEDF data positioning a movable quadrupole mass spectrometer (QMS) along the supersonic jet. This instrument is grounded and has a cylindrical shape (50 mm of diameter), the energy of incoming ions is reasonably the same which they impact onto the substrate during a deposition. We then propose a computational model to simulate the energy evolution of ions moving in the supersonic jet to reproduce the IEDFs based on our experimental observations. We developed a MATLAB code to study argon IEDFs numerically from first principle calculations.

This paper is organized as follows: in the next section we will describe the experimental set-up we used for acquiring experimental data, giving also information about the collection of IED, in section 3 we will explain the physical background of the supersonic jet required to understand the main processes which take place in our reactor and in section 4 describe our approach to simulate ion dynamics. In section 5 the results from experimental data will be shown and compared to our simulations, in section 6 we will introduce the motivations and the computational implementation of charge transfer reactions to obtain more realistic simulations.

2. Experimental set-up

2.1. PA-SJD reactor

The formation of the supersonic jet requires a sufficiently high pressure difference between the inlet and exit orifice of a nozzle. To have a versatile reactor for nanostructured depositions we developed a device divided in two different cylindrical vacuum vessels connected through a nozzle, the layout is sketched in figure 1. The first vacuum chamber is the plasma chamber (95 mm long with 62.5 mm radius), the second is the deposition chamber (200 mm long with 160 mm for inner radius). The pressure ratio between the two chamber $R = p_P/p_D$ can be modified varying the conductance of the main pumping group (a turbomolecular and a rotary pump which let us operate in moderate vacuum conditions), which is located on the bottom of the deposition chamber. On the right side of the deposition chamber there is also an aperture which puts the system in connection with the QMS. The instrument was used to sample the gas from a small conductance (circular orifice with a 0.100 mm diameter size). To obtain clean measurements without high impurity levels it operates at pressure below 10^{-4} Pa granted by a second pumping group (a turbo molecular and a rotary pump). The left lid of the biggest vacuum chamber is in direct contact with the plasma chamber and it contains the inlets for the gas and the precursor for the depositions. The gas is injected from mass-flow controllers ranging from 1.4 to 14 sccm for Ar gas. The lid also has two connections to the inductive antenna (planar copper coil, cooled by deionized water). The pressure in the chambers and the spectrometer is monitored using three capacitance pressure gauges. Their pressure reading precision is good in the working pressure ranges, which are 1-20 Pa in the plasma chamber and 0.1-8 Pa in the deposition chamber.

Inside the plasma chamber a Inductively Coupled Plasma is generated by a 13.56 MHz radiofrequency power generator (Huttinger PFG 1600 RF). The generator is connected through a tunable matching box (L-type) to a two and three quarters loop planar antenna made of copper wire located on the right side of the plasma chamber, inside a teflon scaffold covered by an alumina disc to reduce teflon sputtering. All the chamber is then grounded at the same potential.

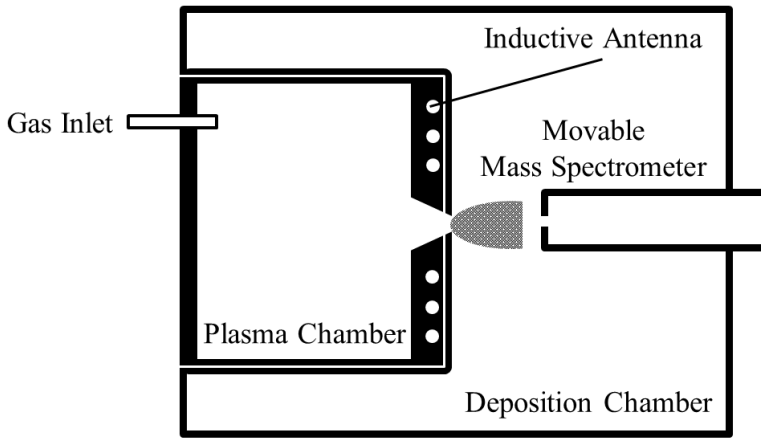

Figure 1. Experimental set-up.

2.2. Quadrupole mass spectrometer
The gas exiting from the plasma chamber can be sampled by the quadrupole mass spectrometer (Hiden EQP-1000 Analyser). This instrument consist of an electron-impact ionization region, an optic system for ion focusing, an high transmission 45° sector field ion energy analyser and a quadrupole mass spectrometer. This QMS is capable of measuring mass and energy spectra allowing detailed analysis of positive ions, radicals and neutrals and it can be moved along the axis of symmetry of the chamber to obtain measurements at different positions along the jet. To measure the IEDFs the QMS operates in this way: the ions produced outside the instrument enter the 0.1 mm sampling orifice with an initial energy E_i and they are immediately focused by a lens into the drift space. In this region they are accelerated to an energy of $E_\mathrm{i} + qV_\mathrm{axis}$, where V_axis is normally set to 40 V. Then the 45° energy filter transmit only ions with the desired energy E. The ions remaining will then be slowed to the transit energy required for the mass scan inside the quadrupole and selected by the mass filter. The detector is a secondary electron multiplier pulse-counting detector which can provide mass spectra in counts/sec over m/z from 0 up to 1000 amu and energy spectra in counts/sec over eV from -100 to 100 eV. The instrument is grounded and uses the deposition chamber as reference potential.

3. Theoretical background
To understand and simulate the dynamics of Ar ions, it is important to make some assumption based on the physics of our system. For this purpose we will here describe in detail firstly the main relations and properties of the supersonic jet and the effects on neutral and ion energies.

Under-expanded free jets have been studied and applied widely in the last decades [12]. A rapid and unconfined expansion of a gas exiting from a sonic orifice into a low pressure chamber creates a supersonic and directed jet. As the volume increases, temperature, pressure and density decrease abruptly according to the laws which describes an isentropic process, thus accelerating the gas particles increasing the Mach number (defined as the ratio between the velocity of a particle and the local sound speed) above 1. The thermal energy of the molecules is converted into flow velocity forming the supersonic jet. The expansion ends with a normal shock, called Mach disc, where temperature, pressure and density reach the background values as the Mach number returns below 1. The properties of this supersonic beam are mainly determined by the size and shape of the nozzle and by the thermodynamic properties of the gas upstream of the nozzle. A schematic representation of the geometry of a supersonic jet is sketched in figure 2.

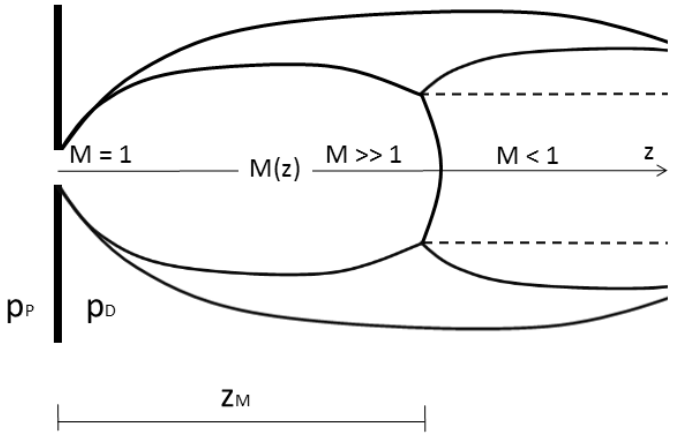

Figure 2. Representation of the supersonic expansion geometry formed after the nozzle exit orifice from the pressure different between the pressure in the plasma chamber, p_P, and the pressure in the deposition chamber, p_D. The shock position, z_M, is indicated and represents the maximum extension of the supersonic jet.

Some useful empirical equations, verified experimentally, can help to reconstruct with good accuracy the geometry of the supersonic jet, for the Mach disc distance from the nozzle z_M we have [13]:

$$\frac{z_M}{D_n} = 0.67\sqrt{R} \tag{1}$$

where D_n is the orifice diameter and R the pressure ratio between the two chambers. In our experimental setup we used a converging nozzle followed by a circular orifice. The converging nozzle favours the formation of the jet, even if it is not fundamental as described in [14]. The exit area of our nozzle is a circular orifice having a 6.9 mm diameter, using the equation for the Mach disc position above and assuming a value of R of 40, we obtain a Mach disc position at about 30 mm, depending on the background pressure we set in the deposition chamber. From [13] it is also possible to obtain some empirical formulas describing the variation of Mach number and pressure along the centerline of the expansion, as a function of the position z and we estimate Mach numbers up to 8 for z about 30 mm. We derived a formula for the variation of density along the jet combining the equation proposed in [15] for the pressure on a flat plate positioned at a certain z with the isentropic relations for an ideal gas obtaining:

$$\frac{n(z)}{n_{\text{Plasma}}} = \left(1.44\left(\frac{z}{D_n}\right)^2 - 0.65\frac{z}{D_n} + 0.87\right)^{-1/\gamma} \tag{2}$$

where γ is the gas adiabatic index. Inside the jet, argon particles are quickly accelerated to a limit velocity which is related to the mass of the gas particles m and its temperature in the plasma chamber T_{Plasma} and asymptotically close to [16]:

$$u_{\text{limit}} = \sqrt{\frac{2\gamma k_B T_{\text{Plasma}}}{(\gamma - 1)m}} \tag{3}$$

which correspond to 746 m/s or 0.114 eV when considering Ar gas at our experimental conditions. The energy gained from the ions is much greater due to the sheath acceleration, so the energy for an ion can be approximated to [9,17]:

$$E_0 = k_B T_e + q(V_P - V(z)) \quad (4)$$

where V_P is the plasma potential inside the plasma chamber (assumed positive and almost constant), $V(z)$ the potential along the jet in the deposition chamber and q the electric charge. The value of E_0 represent the maximum energy achievable, collisions with neutral gas outside the plasma chamber can reduce this energy, slowing down the ions.

4. Computational approach

Our goal is to simulate IEDFs from first principles, introducing model parameters only when it is required to keep the approach tractable and accurate. We developed a MATLAB code to integrate the equations of motion for our interacting system. First of all the role of electrons inside the supersonic expansion can be considered negligible, since they are too fast if compared with ions and atoms (neutrals). The plasma charge density can be assumed much lower than the neutral density allowing us to study the dynamic of a single ion at a time moving through the jet, thus neglecting long range ion-ion interactions. A single simulation provides us the energy of an ion along its trajectory. By performing a large number of simulations (generally hundreds) it is possible to reconstruct histograms representing the IEDFs for different positions. In each simulation the motion from the initial position to the fixed ending point, located several mm away from the starting location, is decomposed into a succession of cylindrical simulation cells. The cylinder (500 μm long and with a radius of 0.004 μm) is filled with neutrals Ar uniformly. The number of neutrals is set according to their density in a supersonic jet given in the previous section.

To further simplify the computational approach we assume that our reference system is moving along the z direction with the velocity of neutrals inside the jet. Thus, neutrals will appear frozen for an ion moving at u_{limit}. When the ion exits the simulation cell, a new cell is constructed, by orienting the axis of the cylinder according to the ion velocity. To describe the interaction between a singly charged ion and a neutral noble gas we use a modified 12-4 Lennard Jones potential [18,19]. This allows the computation of long range collisions by taking into account charge-induced dipole interactions. The equations of motion, determined by this potential, set a system of differential equations which can be numerically solved using a MATLAB algorithm. The interval of integration was set to 0.1 nanoseconds, thus slower ions require much more computation time for each cell. When the ion velocity is comparable with the neutral velocities, the simulation is stopped and the kinetic energy randomly drawn out from a Gaussian distribution centered at E=0.

5. Results

5.1. Experimental work

Experiments were conducted in a argon plasma generated with an inductive coupling. The pressures in the plasma and the deposition chambers were set respectively to 4.5 and 1.4 Pa, obtaining a pressure ratio R of 32 and a corresponding Mach disc distance from the nozzle z_M of 26 mm. The RF input power was then raised gradually up to 450 W, which is the power value also used for thin film depositions [10,11]. We then used the QMS to acquire IEDFs at different positions along the jet, focusing our interest on the study of argon ions.

In the ICP reactor, where the discharge is purely inductive, ions are produced at a uniform and low plasma potential value (generally below 20 eV) and their energy distribution functions exhibit a mono-energetic peak approximatively over the electron temperature kT_e. Upon crossing a collisionless sheath they gain an energy equal to the potential drop [9]. The IEDFs we measured in the deposition chamber are shown in figure 3. Two different energy peaks are clearly distinguishable. The higher peak corresponds to the fast ion population which enters the

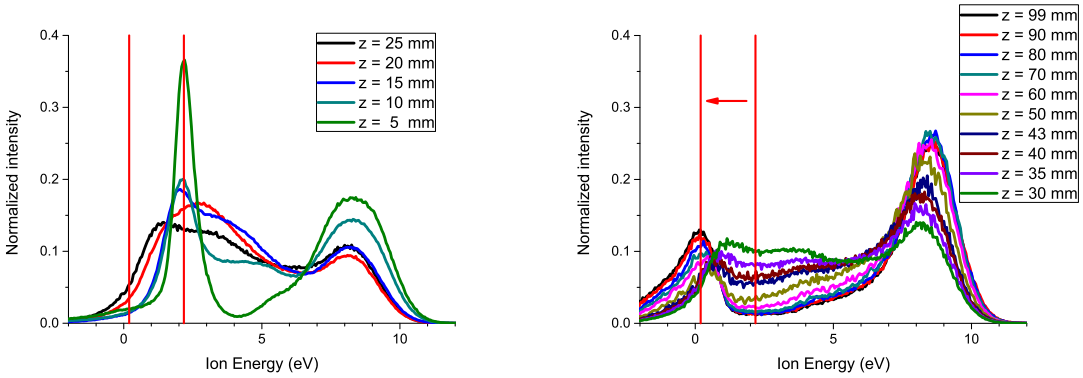

Figure 3. IEDFs measured along the jet (first graph on the left) and after the shock positioned at 26 mm (second graph on the right). Acquired data have been averaged over few measurements cycles and renormalized to have the same total area equal to 1. The red vertical bars indicate the low energy peak at 5 mm and 99 mm from the nozzle.

mass spectrometer without undergoing in any collisional process. The peak is almost stable at 8.3 eV for each position and represent the average maximum energy achievable. The low energy peak is related to collisional processes which take place out of the plasma chamber, it is located at 2.2 eV inside the jet and at 0.2 eV after the Mach disc. Upon crossing the nozzle, ions enter the low-collisional supersonic expansion and are immediately accelerated from potential drop between the plasma potential V_{P} and a the potential along the jet V_{jet}. Inside this region ions can drift and reach the QMS without colliding, maintaining their total energy, or can collide lowering their energies. Since our QMS is grounded and its sheath can be considered almost collision-less, the lowest energy measurable corresponds to strong collisions which reduce the energy to a small kinetic value plus the potential energy V_{jet}. After the Mach disc position the low energy peak drops to lower value, about 0.2 eV, which is comparable with the neutral energy thus indicating a rapid decrease of the potential in this region. Strong collisions seem much favoured in the first part of the jet, but there is also an energy spread and redistribution between the two peaks that corresponds to those ions that collide without losing all their energy. Some energies measured are negative, this is due to ions colliding or formed in the acceleration region of the instrument [20].

5.2. Simulations

From the experimental data collected we gained a good insight on the ion dynamics and the main reaction processes. We have used these information to initialize our simulations and study the effect of collisions along the jet. The initial energy distribution is not trivial to guess or determine without a direct measure: inside the plasma chamber it is reasonably a mono-energetic distribution centered at the higher energy peak measured (8.3 eV), but the evolution of this distribution inside the nozzle inlet region is complicated and depending on many parameters.

We set the initial point of our simulation at 5 mm and extracted initial energies following the IEDF measured experimentally at this position. In figure 4 the simulation values are fitted to the experimental results. They are used as the starting energy distribution values of Ar^+ in the simulations at larger distances. The dynamic of 300 ions was simulated from 5 to 20 mm and compared to our data. Over the z axis we assumed a constant potential centered at V_{jet} set from experimental data about 2 eV. According to this the kinetic energy of a ion is equal to the difference between its initial energy and this potential value $E_i - qV_{\mathrm{jet}}$, while the detected energy is the sum of the two. In figures 4-7 we compare the simulated IEDFs with the measured data

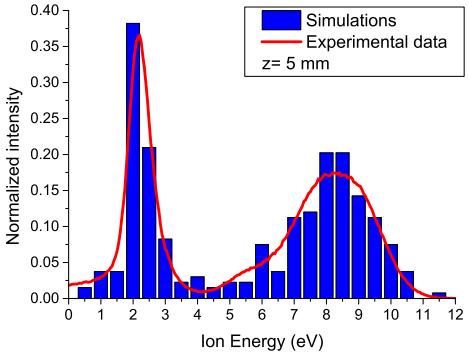

Figure 4. Initial energy distribution.

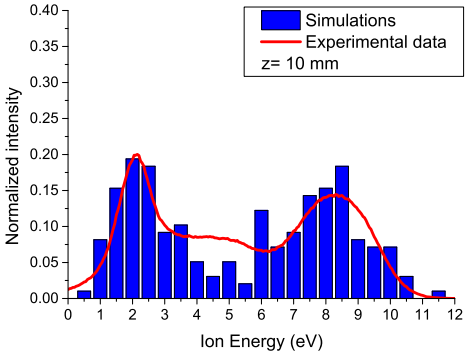

Figure 5. IEDF at 10 mm.

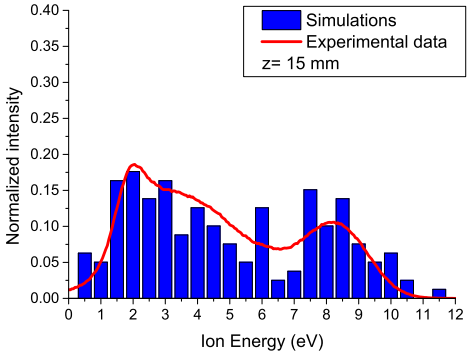

Figure 6. IEDF at 15 mm.

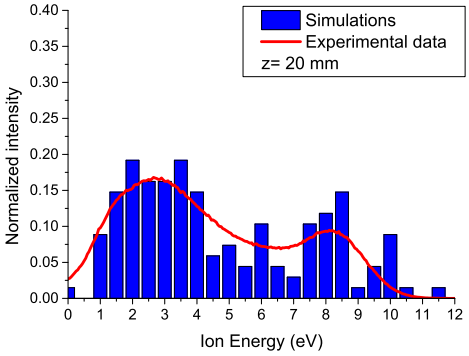

Figure 7. IEDF at 20 mm.

at distances of 10 mm, 15 mm and 20 mm from the nozzle. The simulated data agree quite well with the experimental results. The evolution of the two energy peaks is consistent along z. It is also possible to observe an increase of ion counts in the middle energetic region of the spectra.

6. Charge transfer effects

In the simulations shown in figures 4-7, the only collisional processes considered are elastic collisions between ions and neutrals, treated as dipole interactions. In many experiments with similar plasma sources also charge transfer reactions play an important role especially when happening across the sheath [21,22]. When an ion and a neutral collide, if the distance between the two nuclei is short enough, an electron can be exchanged between them. Charge transfer between argon ions and any nucleus can thus produce fast neutrals and energy losses in the IEDFs, according to the reaction:

$$\mathrm{Ar}^{+}_{\mathrm{fast}} + \mathrm{X}_{\mathrm{slow}} = \mathrm{Ar}_{\mathrm{fast}} + \mathrm{X}^{+}_{\mathrm{slow}} \tag{5}$$

This kind of reaction is very common in plasma, especially with argon, and it has a constant cross section σ at low energies (below hundreds of eV), comparable with the σ for momentum transfer [23]. Experimentally QMS data shown that in argon-oxygen plasma, the Ar^+ signal decreases by 2-3 order of magnitude respect to the value in common argon plasma, suggesting an active charge transfer between argon ions and oxygen neutrals. So we decided to consider also Ar^+-Ar charge transfer reactions in our code with an approximation. An accurate description of

the phenomenon requires a quantum mechanical approach, which is too complicated for multi electrons atoms. In a first approximation the probability that an atom will transfer an electron to an ion decreases exponentially with distance between the atom and the ion.

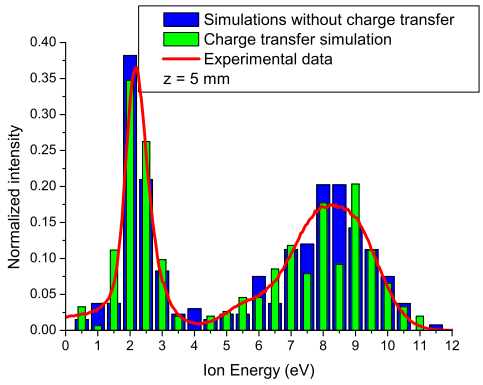

Figure 8. Initial Energy distribution.

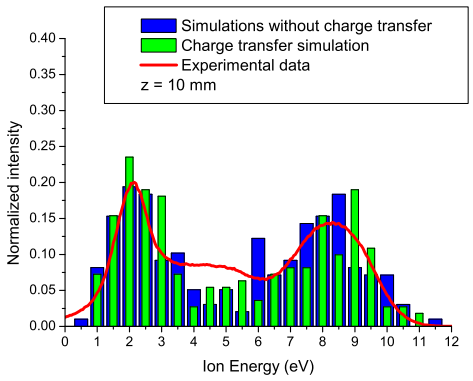

Figure 9. IEDF at 10 mm.

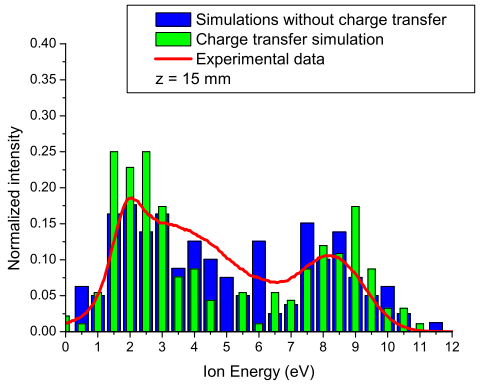

Figure 10. IEDF at 15 mm.

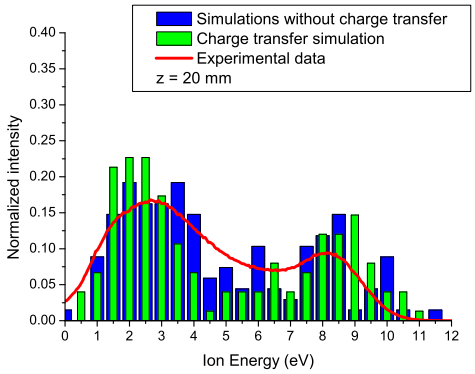

Figure 11. IEDF at 20 mm.

If the ion and the atom approach enough that their electron orbits overlap, then an electron will be exchanged between them many times and, after the collision, it will remain in either of them with equal probability 1/2 [25]. When the inter-atomic distance during a collision is below $r_{\min} = \sqrt{\frac{2\sigma}{\pi}}$, at the end of the collisional process the code considers the neutral atom as the original ion, and vice versa with a given charge transfer probability P_{exchange}. In our code P_{exchange} is equal to 0 when the distance is above r_{min} otherwise it increases exponentially up to 1/2 depending on the energy transferred to the neutrals. In figures 8-11 are shown the results of 300 simulations with charge transfer, compared with both experimental data and simulations without charge transfer. Differences between the initial energy distribution functions in figure 8 are due to statistical fluctuations in the random number generator which can be made smaller by increasing the number of simulations. The addition of charge transfer creates apparently similar IEDFs with a slightly higher low energy peak. However nearly 125 of 300 ions had at least one charge transfer reaction with a neutral atom. In the 180 charge transfer reactions simulated it was possible to calculate the energy loss in the IEDFs, as the difference between the energy of the ion before the collision, and the final energy of the ionized neutral. As shown in figure 12

charge transfer between Ar ions and neutrals in our model introduce in most cases small energy losses.

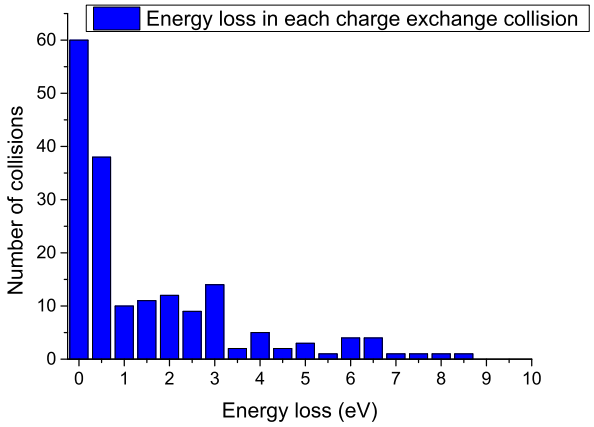

Figure 12. Energy loss in different charge transfer collisions.

7. Conclusions

A model to simulate IEDFs in a low pressure supersonic plasma jet was proposed based on the physics involved. Experimental measurements were performed in argon plasma using a QMS to acquire ion energy spectra along the jet. The results show an interesting two peaked distributions and were used to develop a simulation code which integrates the equations of motion from first principles. It was possible to simulate the dynamics of ions moving along the jet under some assumptions made from experimental observations or theory in order to reproduce the measured data. The agreement between the data and simulations is very good.

Charge transfer reactions have been taken into account in an approximate fashion by using two parameters, one representing a cut-off distance (see e.g. [23]) within which the reaction can occur, and a second one representing an energy threshold on the impact energy transferred to the neutral atom. The present results indicate that charge transfer occurs at least once in about 40% of the total ion trajectories simulated. Yet, they suggest that the corresponding effects are not important in determining the global shape of the IEDFs in the case of argon.

References

[1] Petrov I, Hultman L, Helmersson U, Sundgren J E, Greene J E, 1989 *Thin Solid Films* **169**, 299
[2] Mattox D M, 1989 *J. Vac. Sci. Technol. A* **7** No.3, 1105
[3] Profijt H B, Kessels W M M, 2012 *ECS Transactions* 50 **13**, 23
[4] Hippler H, Kredl J, Vartolomei V A, 2009 *Vacuum* **83**, 732
[5] Malakhovskii A, 1999 *Phys. Chem. Chem. Phys.* **1**, 4187
[6] Logue D M, Shin H, Zhu W, Xu L, Donnelly V M, Economou D J, Kushner M J, 2012 *Plasma Sources Sci. Technol.* **21**, 065009
[7] Lee J B, Chang H Y, Seo S H, 2013 *Plasma Sources Sci. Technol.* **22**, 065008
[8] Kawamura E, Vahedi V, Lieberman M A, Birdsall C K 1999 *Plasma Sources Sci. Technol.* **8**, R45
[9] Kortshagen U, Zethoff NI, 1995 *Plasma Sources Sci. Technol.* **4**, 541
[10] Trifiletti V, Ruffo R, Turrini C, Tassetti D, Brescia R, Di Fonzo F, Riccardi C, Abbotto A 2013 *J. Mater. Chem.* A **1**, 11665
[11] Biganzoli I, Fumagalli F, Di Fonzo F, Barni R, Riccardi C 2012 *J. Mod. Phys.* **3**, 1626
[12] Fenn J B, 2000 *Int. J. Mass Spectrom* **200**, 459
[13] Ashkenas H, Sherman F 1966 *Rarefied Gasdynamics* **4**, Academic Press, New York

[14] Murphy H R, Miller D R 1984 *J. Phys. Chem.* **88** No.20, 4474
[15] Abouali O, Saadabadi S, Emdad H 2011 *J. Aerosol Sci.* **42** 65
[16] Huang C, Nichols W T, O'Brien D T, Becker M F, Kovar D, Keto J W, 2007 *J. Appl. Phys.* **101**, 064902
[17] Tanner S D, 1993 *J. Anal. At. Spectrom.* **8**, 891
[18] Chen W L T, Heberlein J, Pfender E 1996 *Plasma Chem. Plasma Process.* **16** No. 4, 635
[19] Michels H H, Hobbs R H, Wright L A 1978 *J. Chern. Phys.* **69**, No.11 , 5151
[20] Olthoff J K, Van Brunt R J, Radovanov S B 1995 *Appl. Phys. Lett.* **67** No.4 , 473
[21] Babaeva N Yu, Lee J K, Shon J W, Hudson E A 2005 *J. Vac. Sci. Technol.* A **23**, No. 4, 699
[22] Barton D, Bradley J W, Steele D A, Short R D 1999 *J. Phys. Chem.* B **103**, 4423
[23] Phelps A V 1991 *J. Phys. Chem. Ref. Data* **20**, No. 3, 557
[24] Maiorov S A, 2009 *Plasma Phys. Rep.* **35**, No. 9, 802